Physica A 413 (2014) 31–41

Contents lists available at ScienceDirect

Physica A

journal homepage: www.elsevier.com/locate/physa

Absorption spectra and localization aspects of a one-dimensional model with stretched exponential correlated disorder

J.L.L. dos Santos, M.O. Sales, F.A.B.F. de Moura *

Instituto de Física, Universidade Federal de Alagoas, Maceió - AL 57072-970, Brazil

HIGHLIGHTS

- Localization and correlated disorder.
- Dependence of the absorption spectrum on the degree of correlations.
- Direct relation between absorption spectrum intensity and the localization length.

ARTICLE INFO

Article history:
Received 7 February 2014
Received in revised form 18 June 2014
Available online 5 July 2014

Keywords:
Localization
Correlated disorder
Absorption spectrum
Exciton

ABSTRACT

In this paper, we numerically analyze the dynamics of a one-electron in a one-dimensional model with stretched exponential correlations in the diagonal disorder distribution. We analyze in detail the effect of this correlated disorder on the localization aspects and the optical absorption. We offer an estimate for the localization properties and its dependence on the intrinsic correlations in the disorder distribution. Our calculations of the optical absorption spectra suggest that as the disorder distribution becomes more correlated the absorption intensity decreases. We explain this behavior in detail by using heuristic arguments.

1. Introduction

P.W. Anderson and co-workers proved by using scaling theory that extended eigenstates are absent in low-dimensional systems with uncorrelated disorder [1–5]. Since the end of the eighties, it was shown that low-dimensional disordered systems can support extended states or a localization–delocalization transition in the presence of short- or long-range correlations in the disorder distributions [6–30]. From the experimental point of view, V. Bellani et al. [16] and U. Kuhl et al. [19] have studied the effect of short- and long-range correlations on the transport properties of low-dimensional disordered systems. Moreover, it was suggested that an algorithm for generating random correlated sequences with desired mobility edges could be used in the manufacture of filters for electronic or optical signals [13]. Furthermore, the theoretical prediction that it is possible to *see* Anderson localization in a random multilayer filter [31] opened a wide field of investigations of effects of correlated disorder in optical systems.

In the recent years, a key problem in the context of condensed matter physics is to understand what is the effect of correlated disorder on the optical spectroscopy properties [32–42]. Usually, it is well known that optical spectroscopy fails in detecting localization–delocalization transitions. However, in Ref. [35] an anomalous behavior of the absorption

* Corresponding author. Tel.: +55 8299593909.
E-mail address: fidelis@fis.ufal.br (F.A.B.F. de Moura).

http://dx.doi.org/10.1016/j.physa.2014.06.049
0378-4371/

spectrum in a one-dimensional ($1d$) lattice with long-range correlated diagonal disorder was reported. It was found that long-range correlated diagonal disorder promotes the appearance of an absorption spectrum profile with two peaks [35]. Moreover, it was proposed to use this double-peak absorption spectrum as a spectroscopic tool to monitor the Anderson transition [35]. Furthermore, in Ref. [39] a double-peak absorption spectrum was numerically observed in a $1d$ lattice with long-range off-diagonal correlated disorder. In Ref. [40], a detailed study of the optical properties in $1d$ models with heavy-tailed Levy disorder distribution was done. The authors found a broadening of the optical line and a non universal scaling of the distribution of exciton localization lengths. The scaling of the optical absorption bandwidth and the non universality of the localization length within models with Levy disorder distribution were re-visited in Ref. [41]. In general, the study of the dependence of the absorption spectrum on the properties of the disorder distribution give us key information that can be used to study the nature of eigenstates.

In this paper, we report further progress along these above lines. We will study the problem of one-electron localization and optical absorption spectrum in $1d$ systems with correlated disorder. Our calculations were carried out on open chains with stretched exponential correlations in the disorder distribution. We perform exact numerical diagonalization to compute the participation number and the optical absorption spectrum. Our formalism provides an estimate for the dependence of the localization length on the type of correlated disorder considered here. In general, the localization length increases as the generalized correlation length is increased; however, we have not found a localization–delocalization transition. Our results for the optical absorption spectra reveal an interesting dependence of the absorption spectrum on the correlated disorder distribution. We observe that as the disorder distribution becomes more correlated the absorption intensity is decreased. We will explain this behavior in detail by using heuristic arguments. We obtain a simple relation between the optical absorption intensity and the localization length around the specific eigenstates with largest oscillator strength. Numerical calculations of the optical absorption and the localization length give support to our heuristic arguments.

2. Model and formalism

We consider the disordered Anderson model defined by the one-electron Hamiltonian [1,2,4,29]

$$H = \sum_{n=1}^{N} \epsilon_n |n\rangle\langle n| + t \sum_{\langle n,m\rangle} |n\rangle\langle m|, \tag{1}$$

where $|n\rangle$ is a Wannier state localized at site n and $\sum_{\langle n,m\rangle}$ represents a sum over nearest-neighbor pairs. Hereafter we will use energy units of $t = 1$. ϵ_n represents the on-site disorder distribution. We will consider open boundary conditions. In our work, we are interested in studying the nature of the eigenstates and the optical absorption spectrum by analyzing the above Hamiltonian in the presence of an on-site disorder distribution with stretched exponential correlations. The on-site potential ϵ_n with stretched exponential correlations will be generated by using the following formalism: initially we will calculate the sequence E_n defined by

$$E_n = \sum_{m=1}^{N} \eta_m * \exp(-|n-m|^{\gamma}/\zeta) \quad n = 1, \ldots, N \tag{2}$$

where η_m are independent random numbers uniformly distributed in the interval $[-0.5, 0.5]$ and γ and ζ are tunable parameters that control the degree of correlations. The on-site potential ϵ_n is obtained by using the formula

$$\epsilon_n = [E_n - \langle E_n\rangle]/\sqrt{\langle E_n^2\rangle - \langle E_n\rangle^2} \quad n = 1, \ldots, N. \tag{3}$$

Therefore, the diagonal disorder displays zero mean value ($\langle\epsilon_n\rangle = 0$) and fixed standard deviation ($\sqrt{\langle\epsilon_n^2\rangle - \langle\epsilon_n\rangle^2} = 1$). Let us discuss now some properties associated with the parameters γ and ζ. We will also discuss the values of γ and ζ that will be considered in our work. We can see that, for a fixed γ, the degree of correlations within the disorder distribution increases as ζ is increased. ζ is a type of generalized correlation length, and it can be used as a way to quantify the degree of correlation within the disorder distribution; however, formally, it is not the correlation length. Only for $\gamma = 1$ the ζ parameter has the status of the standard correlation length. We also emphasize that for $\gamma = 1$ the disorder distribution is exactly the same that was investigated in Ref. [29]. For a fixed value of $\zeta > 0$ and for $\gamma = 0$ there is no disorder at the sequence defined by Eq. (2). Therefore, the rescaling defined in Eq. (3) cannot be used in this case. In our study, we will focus our calculations on the disordered case ($\gamma > 0$). We observe that the internal correlations within the on-site energy distribution decrease substantially at the limit of large γ. From another side, for small γ, the decay of the correlation function becomes slower. Therefore, we will analyze the nature of the electronic eigenstates and the optical response at both limits: the case with weak correlations ($\gamma \gg 1$ and $\zeta \to 0$) and also the case with strong correlations ($0 < \gamma < 1$ and $\zeta \gg 0$). In Fig. 1(a) (left panel) we plot the on-site energy ϵ_n versus n for $N = 10^5$, $\zeta = 10$ and $\gamma = 0.25, 0.5, 0.75$ and 1.25. One can notice how the energy landscape becomes smooth as γ decreases. In order to compare some statistical properties of the above sequences, we compute the auto-correlation function ($C(r) = [1/(N-r)] * \sum_{n=1}^{N-r} \epsilon_n\epsilon_{n+r}$) of the potential landscape (see Fig. 1(b) (right panel)). Circles indicate the numerical calculation of $C(r)$ and the solid line represents

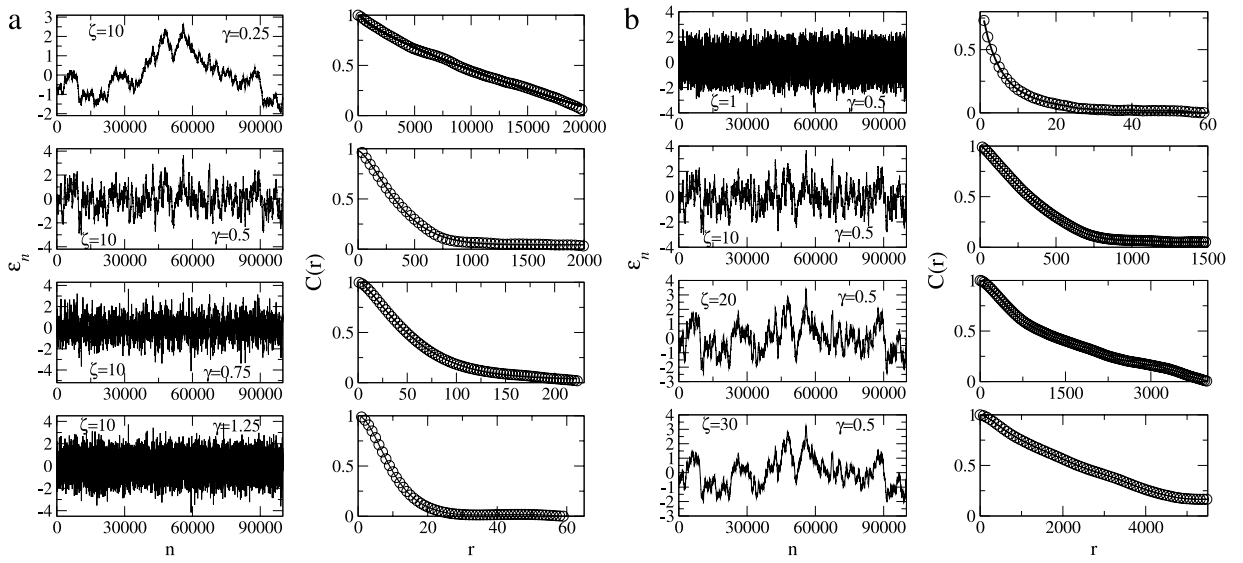

Fig. 1. (a) Left panel: typical on-site energy landscapes generated from Eqs. (2) and (3) with $N = 10^5$, $\zeta = 10$ and $\gamma = 0.25$, 0.5, 0.75 and 1.25. Right panel: numerical calculation of the respective two-point auto-correlation function (circles) and the solid line represents a numerical fit using a stretched exponential form. (b) Left panel: same as in left panel (a) with $N = 10^5$, $\gamma = 0.5$ and $\zeta = 1$, 10, 20 and 30. Right panel: same as in right panel (a) for $\gamma = 0.5$ and $\zeta = 1$, 10, 20 and 30.

a numerical fit using a stretched exponential form. In Fig. 1(b) we plot the same as in (a) for fixed $\gamma = 0.5$ and $\zeta = 1, 10, 20$ and 30. We can see in Fig. 1(a, b) that the on-site energy profile and its auto-correlation function are in good agreement with our previous comments about the parameters γ and ζ. We observed that as γ is increased, the auto-correlation function exhibits a faster decay with the distance r (see Fig. 1(a) (right panel)). Moreover, for large γ the on-site energy displays a profile more rough if compared with cases of small γ. The smoothing of the on-site energy profile as γ is decreased is also in good agreement with our previous comments about the dependence of internal correlations on γ. In Fig. 1(b) (right panel) we observe that the auto-correlation function exhibits slower decay with the distance r as ζ is increased. The eigenstates $|\Phi(E)\rangle = \sum_{n=1}^{N} f_n(E)|n\rangle$ can be found by exact diagonalization of the complete Hamiltonian. In our calculations we compute the average of the participation number, defined by [2,9,10]

$$\xi(E) = 1/\sum_{n=1}^{N} f_n^4(E). \tag{4}$$

In general, the participation number is a good estimate of the number of sites that participate in the eigenstate. For extended states, ξ is proportional to the total number of sites ($\xi \propto N$). For localized states, the participation number is finite, therefore smaller than the system size N. A good way to distinguish the nature extended or localized of an eigenstate is to analyze the scaled participation number ξ/N. If ξ/N goes to zero as N is increased we are dealing with localized states. However, if $\xi/N \to$ constant for large N we have strong evidence of extended modes. In addition, we will also focus on the numerical calculation of the localization length λ, done by using the standard transfer matrix procedure [2]. The localization length λ is defined by [2]: $\lambda = \{\lim_{N\to\infty}(1/N)\log[|Q_N F(0)|/|F(0)|]\}^{-1}$ where $F(0) = \begin{pmatrix} f_1 \\ f_0 \end{pmatrix}$ is a generic initial condition and Q_N is the product of all transfer matrices

$$Q_N = \prod_{n=1}^{N} \begin{pmatrix} E - \epsilon_n & -1 \\ 1 & 0 \end{pmatrix}. \tag{5}$$

Furthermore, we will investigate the absorption spectrum defined as [35,36,39]

$$A(E) = \frac{1}{N}\sum_{\beta} \delta(E - E_\beta) F_\beta, \tag{6}$$

where F_β is the oscillator strength associated with the eigenvalue β, namely $F_\beta = [\sum_n f_n(E_\beta)]^2$. For off-diagonal terms positive ($t > 0$) and the diagonal disorder following an uncorrelated distribution, the eigenstates with the largest oscillator strength are those of the top of the band. This formalism was well explained in Ref. [36]. We are considering the interaction of our $1d$ model with the transverse radiation field. The coupling of the radiation field mode of wave vector k with the eigenstate ($|\phi_\beta\rangle = \sum_n f_n(E_\beta)|n\rangle$) is proportional to $\sum_n f_n(E_\beta)\exp(-kr_n)$. In our formalism, we will restrict our study to

system sizes N small compared to an optical wavelength (i.e. $kN \ll 1$). Therefore, the coupling with external field reduces to the transition dipole $\sum_n f_n(E_\beta)$. Therefore, the oscillator strength associated with the one-photon absorption is then proportional to $(\sum_n f_n(E_\beta))^2$.

3. Results

We applied an exact diagonalization procedure on finite chains. All calculations were averaged over, at least, 1000 disorder configurations. We will start by analyzing the localization properties around the center of the band ($E = 0$). We emphasize that the band center $E = 0$ represents the mode with the largest localization length even in the case of the 1d Anderson model with an uncorrelated diagonal disorder distribution [2]. We will emphasize again the physics motivation behind the range of parameters γ and ζ analyzed in our work. We will analyze the nature of the electronic eigenstates and the optical response of our disordered model at the limits of weak and strong correlations. The case with weak correlations is obtained for large γ and small ζ ($\gamma \gg 1$ and $\zeta \to 0$). From another side, the case with strong correlations is obtained for small γ and large ζ ($0 < \gamma < 1$ and $\zeta > 0$). In Fig. 2 we show the participation number at the center of the band ($E = 0$) versus γ for $\zeta = 0.1$, 1, 10 and 20. For $\zeta = 0.1$ we are dealing with a disordered potential with weak correlations. In fact, it is almost the uncorrelated limit. Therefore, the participation number should not change as the γ exponent is varied. This behavior can be observed in Fig. 2(a). One can notice that $\xi(E = 0)$ does not depend on γ. For the correlated case $\zeta = 1$, 10 and 20 we observe an interesting and non-monotonic behavior. For γ within the particular interval $[\gamma_1, \gamma_2]$ the participation number becomes almost of the same order of magnitude of the system size N. We also observe that within these intervals $[\gamma_1, \gamma_2]$ the participation number displays a more intense dependence on the system size N. However, we emphasize that we cannot anticipate the dependence of the participation number on the system size ($\xi \propto N^{D_d}$) from the data we have shown until now. The finite size scaling of the participation number will be obtained later by using a careful analysis of ξ versus N within the intervals $[\gamma_1, \gamma_2]$. For $\zeta = 1$ we can see this behavior within the interval $[\gamma_1, \gamma_2] \approx [0.07(2), 0.23(2)]$ and for $\zeta = 10$ and 20 $[\gamma_1, \gamma_2] \approx [0.10(3), 0.50(3)]$. For $\zeta = 10$ and 20 we will analyze the dependence of the participation number on the system size N in Fig. 2(e). Symbols represent the data and the solid line a power-law fitting ($\langle\xi\rangle_{0.1<\gamma<0.5}/N \propto N^{-0.10(1)}$ for $\zeta = 10$ and 20). Our results suggest that the scaled mean participation number within the region $0.1 < \gamma < 0.5$ ($\langle\xi\rangle_{0.1<\gamma<0.5}/N$) decreases as N is increased thus indicating localized states. In Fig. 3(a–d) we show the localization length around the center of the band ($\lambda(E = 0)$) versus γ for $N = 10^5$, 2×10^5, 4×10^5 and $\zeta = 0.1$, 1, 10 and 20. The results for λ are qualitatively in good agreement with the previous calculations of the participation number. For $\zeta = 1$, 10 and 20 we observed again a non monotonic behavior similar to that observed in Fig. 2(b–d). For γ within intervals similar to those that were obtained in Fig. 2(b–d) the localization length λ also increases. The dependence of the localization length λ on the system size N needs a more detailed study. In Fig. 3(e) we plot the logarithm of the scaled mean localization length within the interval [0.1, 0.5] ($\log\langle\lambda\rangle_{0.1<\gamma<0.5}/N$) versus the logarithm of the system size N. Symbols represent the data and the solid line a power-law fitting ($\langle\lambda\rangle_{0.1<\gamma<0.5}/N \propto N^{-0.25(2)}$). Therefore, in good agreement with the calculations shown in Fig. 2(e), our finite size scaling indicates that the localization length is finite at the thermodynamic limit thus indicating localized states. We recognize that we are unable to obtain a precise estimate of the intervals $[\gamma_1, \gamma_2]$. We emphasize that the intervals reported are rough estimates. The non monotonic behavior of the participation number ξ and localization length λ with γ (see Fig. 2(c–d) and 3(c–d) respectively) needs a more detailed description. We stress that for $\gamma \to 0$ there is an increase of the correlations within the disorder; therefore, the degree of localization should decrease. However, in our calculations, we observe a decrease of the participation number and the localization length as $\gamma \to 0$, i.e. we obtained an increase of the degree of localization. In order to understand better these results we will use an effective measure for the roughness of the diagonal disorder of our chain. Following Ref. [43,44] we will consider the integrated Fourier transform (IFT) defined by $IFT = \int_0^{k_{\max}} \epsilon_k dk$ where ϵ_k represents the Fourier transform of the on-site disorder distribution ϵ_n. For an uncorrelated random diagonal distribution we will have a large IFT due to its noise-like behavior. From the other side, more regular structures will display a narrower Fourier spectrum and therefore a smaller IFT. In Fig. 4 we plot our results for the IFT versus γ for $\zeta = 1$, 10 and 20. We also observe a non monotonic behavior of the integrated Fourier transform. The IFT displays a plateau within the interval $[\gamma_1, \gamma_2]$. The decrease of IFT within the interval $[\gamma_1, \gamma_2]$ indicates that the correlation at this regime effectively decreases the strength of disorder thus giving rise to the increase of localization length. Our results for the IFT are in good agreement with the participation number calculations of Fig. 2(b–d). In special the interval $[\gamma_1, \gamma_2]$ obtained using IFT data fits reasonably the region with large localization length obtained in Fig. 2(b–d) (i.e. $[0.07(2), 0.23(2)]$ for $\zeta = 1$ and $[0.10(3), 0.50(3)]$ for $\zeta = 10$ and 20). We also observe that the IFT increases as $\gamma \to 0$ thus indicating an increase of the roughness within the disorder distribution. It is an apparent contradictory result with the correlation function properties at this limit of small γ. However, we stress that we are using the rescaling defined in Eq. (3). Therefore, this rescaling promotes the increase of roughness for small γ and therefore the decrease of participation number observed in Fig. 2(b–d).

We will investigate now the dependence of the localization properties on the generalized correlation length ζ. We will focus on the scaled participation number ξ/N versus ζ for $E = 0$, $\gamma = 0.3$ and $N = 15{,}000$, 30,000 and 60,000 sites (see Fig. 5). We chose $\gamma = 0.3$ because, as we noted in Fig. 3(c, d), around this value we found the eigenstates with the largest participation number. We stress that for extended states, the function ξ/N from distinct chain sizes would collapse into a

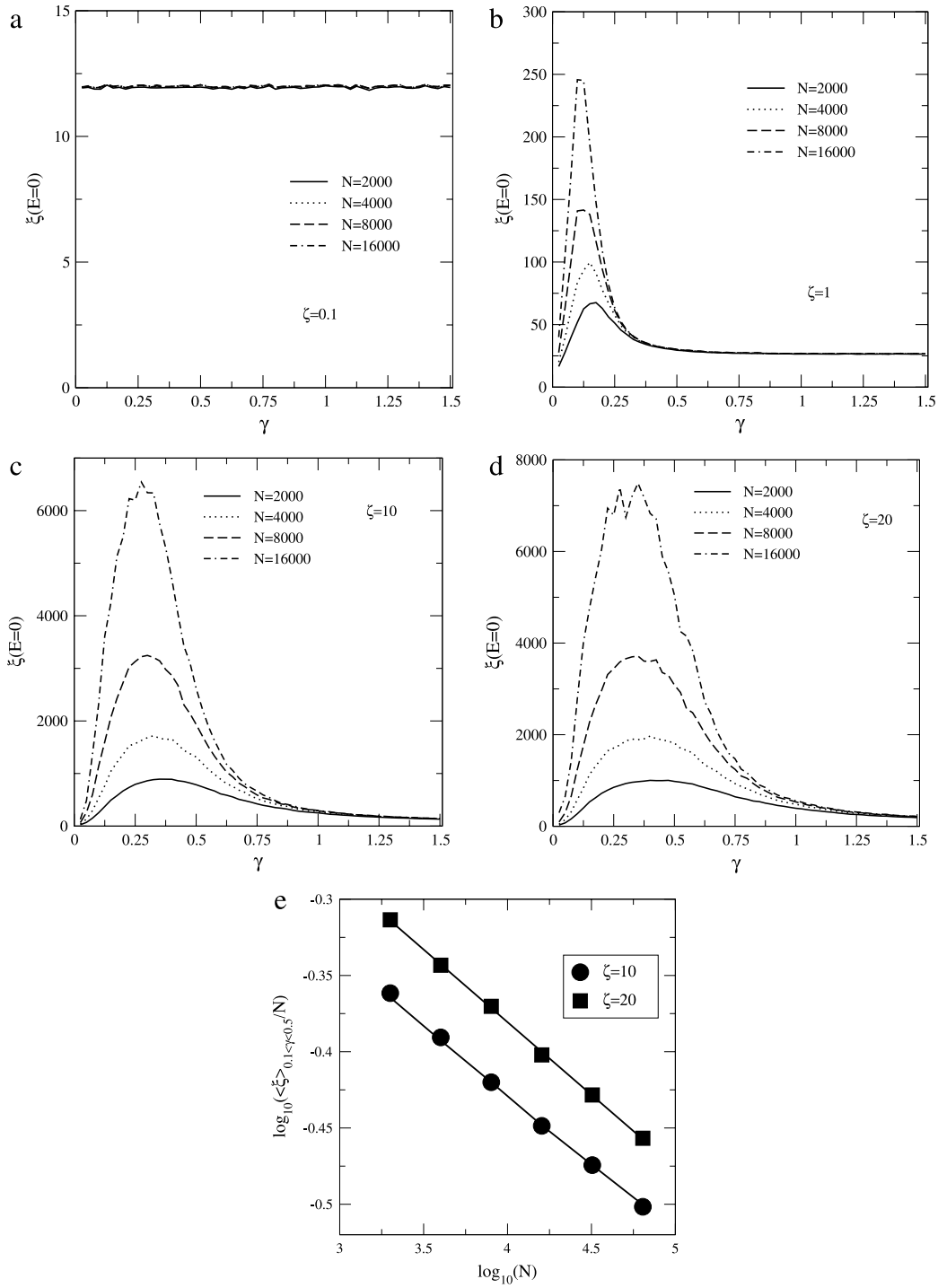

Fig. 2. (a–d) Participation number at the band center ($E = 0$) versus γ for $\zeta = 0.1$, 1, 10 and 20. (e) Log–log plot of the mean participation number within the interval [0.1, 0.5] ($\langle \xi \rangle_{0.1<\gamma<0.5}$) versus the system size N.

single curve, signaling extended states with $\xi \propto N$. In our case, the calculations show no data collapse. Therefore, even for large ζ, the scaled participation number ξ/N decreases as the system size increases, pointing to a localized character of the eigenstates in the thermodynamic limit.

Now, let us show our results for the absorption spectrum of this model. In Fig. 6(a, b, c) we plot $A(E)$ versus energy E for $\gamma = 0.35$ (panel (a)), $\gamma = 0.5$ (panel (b)), $\gamma = 1$ (panel (c)) and $\zeta = 0.01$, 0.1, 0.3, 0.5, and 0.7. Our calculations were done for $N = 2000$ sites and 1200 realizations of disorder. For $\zeta = 0.01$ we observe a peak slightly above the largest

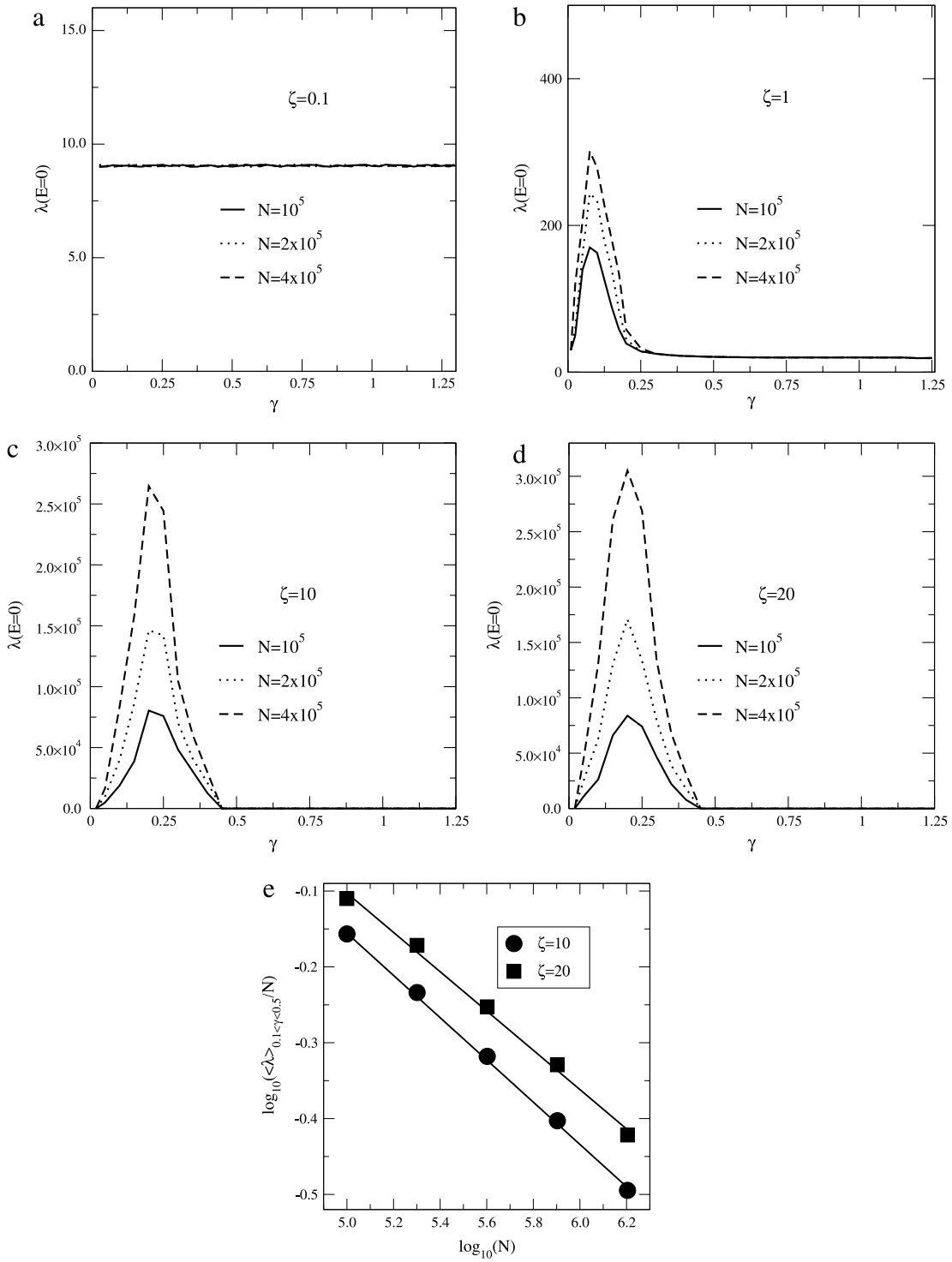

Fig. 3. (a–d) Localization length λ at the band center ($E = 0$) versus γ for $\zeta = 0.1$, 1, 10 and 20. (e) Log–log plot of the mean localization length within the interval [0.1, 0.5] ($\langle\lambda\rangle_{0.1<\gamma<0.5}$) versus the system size N.

band edge $E = 2$ of the periodic lattice. This result is easily understood by remembering that for $\zeta = 0.01$ we are dealing with an uncorrelated diagonal disorder. In $1d$ systems with uncorrelated diagonal disorder and positive hopping only the states around the top band edge contribute to the absorption spectrum [35–37,39]. Our calculations for $\zeta = 0.01$ are in good agreement with these previous results. Now we will increase the parameter ζ. We observe that as ζ is increased the

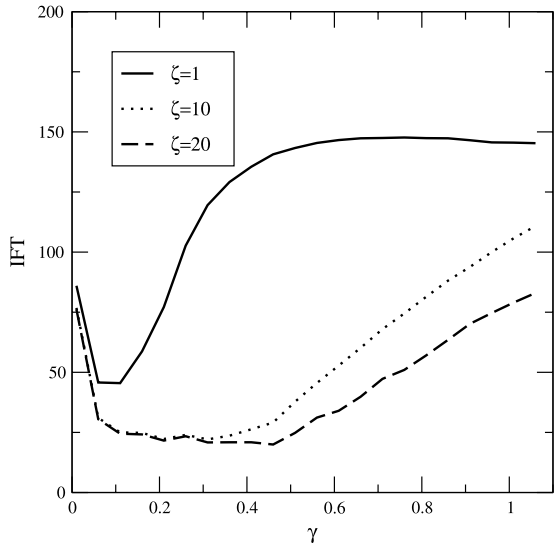

Fig. 4. The integrated Fourier transform (*IFT*) versus γ for $\zeta = 1$, 10 and 20.

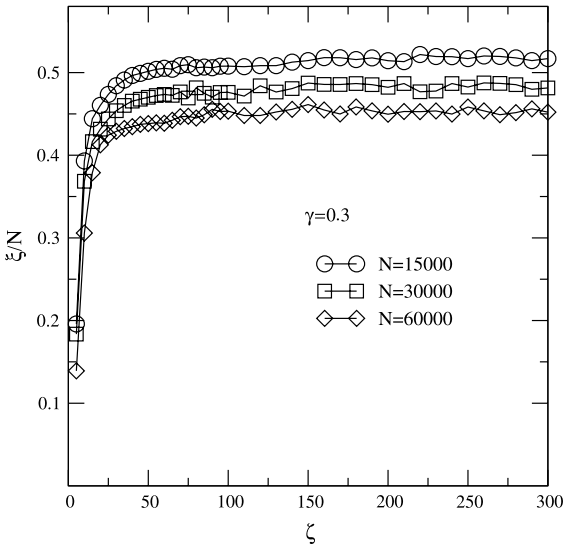

Fig. 5. Scaled participation number ξ/N versus ζ. Calculations were done for $E = 0$, $\gamma = 0.3$ and $N = 15{,}000$, 30,000 and 60,000.

absorption spectrum $A(E)$ becomes wider and its intensity decreases. Therefore, for $\zeta > 0$ we observe an increase of the absorption bandwidth. We stress that an increase of the absorption bandwidth was observed previously in other works with correlated disorder [32,33,35,38]. We emphasize that the correlated disorder distributions considered in Refs. [32,33, 35,38] were quite distinct from that we have considered in our present work. In Fig. 6(d) the standard deviation σ_A of the absorption spectra is shown as a function of the generalized correlation length ζ. To accurately determine the standard deviation σ_A we fitted the high-energy side of the absorption spectra using Gaussians. We observe that σ_A monotonously increases as ζ is increased and saturates for $\zeta > 1$. The limiting value of σ_A displays a weak dependence on the γ exponent; however, in all γ considered, we observed $\sigma_A \propto \zeta$ before the saturation (see the inset). We also observe that the limiting value of σ_A is roughness $\langle\sigma_A(\zeta \to \infty)\rangle \approx 0.9$. This value is quite close to the standard deviation $\sigma = 1$ of the on-site disorder distribution. We stress that in Ref. [33] the authors have reported that the width of the absorption spectrum should converge to the standard deviation of the disorder distribution. We have obtained approximately this behavior in our model i.e. $\sigma_A \approx \sigma$. However, the authors in Ref. [33] also demonstrated the existence of a particular dependence of σ_A on the degree of correlations. The authors demonstrate the presence of a crossover at the limit of strong correlations. In our model we did not find the same behavior reported in Ref. [33]. We stress that in our model we are dealing with a stretched exponential correlated disorder with standard deviation $\sigma = 1$. The correlated disorder used in Ref. [33] consisted of $S = N/N_c$ consecutive segments with equal energies ϵ_s within each segment. The set $\{\epsilon_s\}_{s=1}^{S}$ was chosen as statistically independent

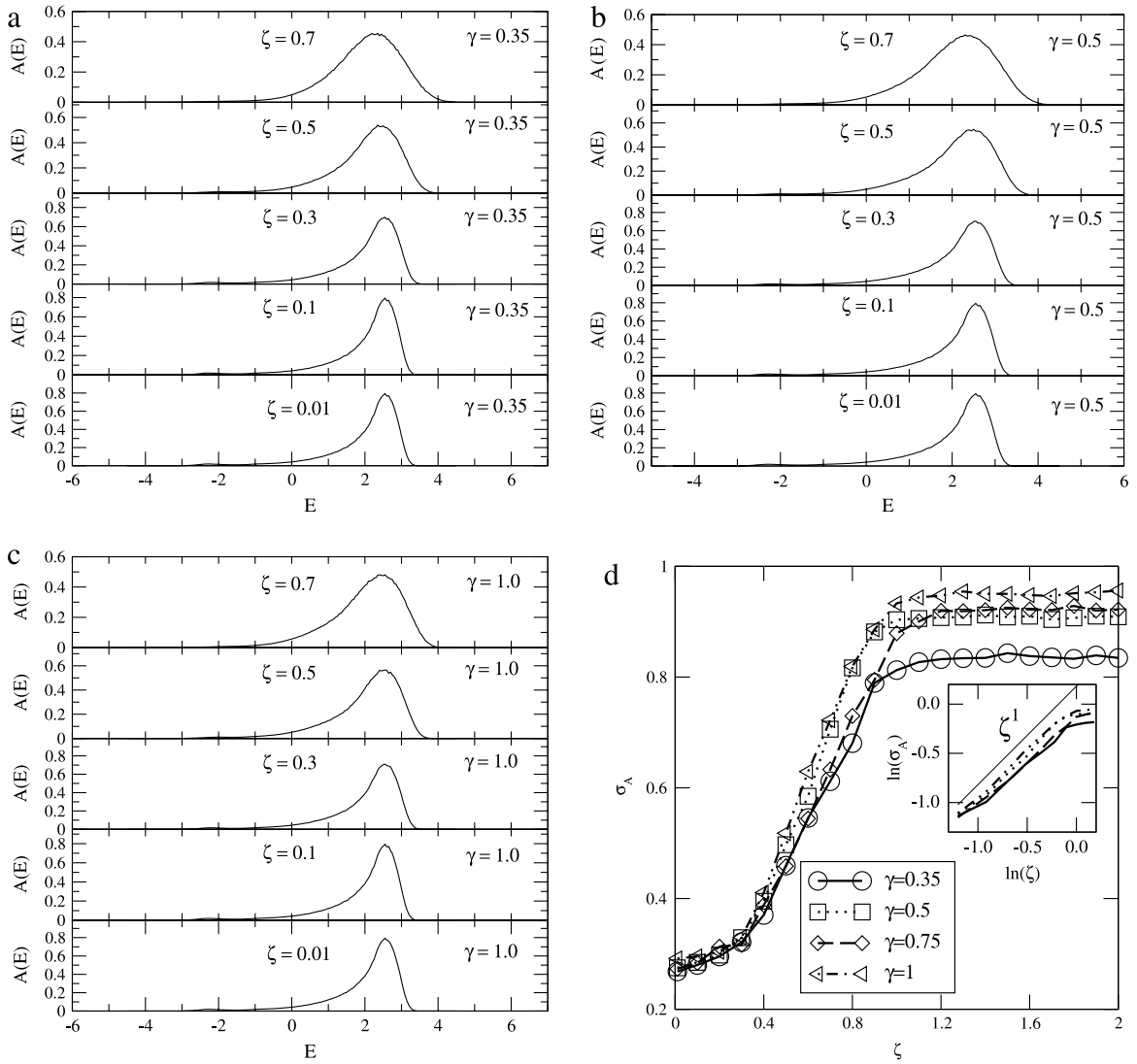

Fig. 6. (a–c) Absorption spectrum $A(E)$ versus energy E for $\gamma = 0.35$ (panel (a)), $\gamma = 0.5$ (panel (b)) and $\gamma = 1$ (panel (c)). Calculations were done for $N = 2000$ sites, 1200 realizations of disorder and $\zeta = 0.01$, 0.1, 0.3, 0.5, and 0.7. (d) The standard deviation σ_A of the absorption spectrum $A(E)$ versus the generalized correlation length ζ.

Gaussian variables with probability distribution $P(\epsilon_s) \propto \exp(-\epsilon_s^2/2\Sigma^2)$. The correlation length in Ref. [33] was well defined as N_c; however, the functional form of the correlation function was not defined clearly. The authors in Ref. [33] have defined the probability distribution within the disorder distribution however, they did not define the type of correlation function was considered. Moreover, the disorder degree used in our manuscript ($\sigma = 1$) is larger than the value considered in Ref. [33] ($\sigma = 0.2$). We will provide some additional numerical calculations to investigate some specificities of the optical properties in the vicinity of the band edge $E = 2$. We will show that the decreases of intensity of the absorption spectrum $A(E)$ can be explained by analyzing the localization aspects at the band edges. In the following we will show new numerical and heuristic analytical calculations that explain in detail the behavior of $A(E)$ in this $1d$ model with short-range correlated disorder. The localization length λ around $E = 2$ decreases as the on-site potential becomes more correlated [45]. In our model, $\lambda(E \approx 2)$ will decrease as the generalized correlation length ζ is increased. This anomalous behavior of λ around $E \approx 2$ explains qualitatively the enlargement of the absorption spectrum band around $E \approx 2$. Following Ref. [35], it was known that the stronger localization at the band edges promotes a spread in the absorption bandwidth. We are interested in giving additional quantitative information of the absorption spectrum and its dependence on the localization degree around $E \approx 2$. Let us consider the mean localization length around $E = 2$ ($\lambda(E \approx 2)$) versus the generalized correlation length ζ. To compute the mean localization length we use the arithmetic average within the interval [1.6, 2.4]. We stress that within this interval, the localization length displays the anomalous behavior reported in Ref. [45]. Results are shown in Fig. 7(a). Now, let us consider in Fig. 7(b) the maximum intensity of the absorption spectrum $A_{\max}$ versus the generalized correlation length

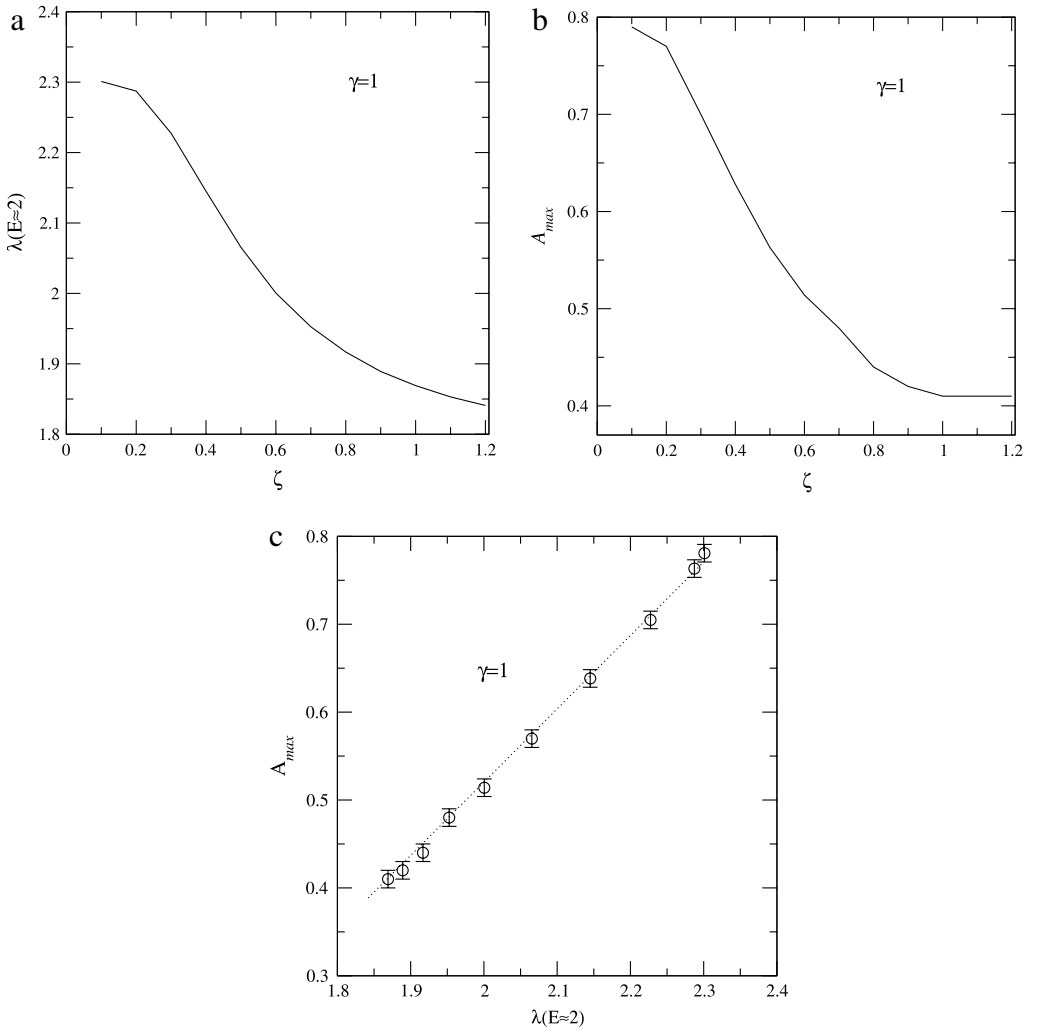

Fig. 7. (a) Mean localization length around $E = 2$ ($\lambda(E \approx 2)$) versus the generalized correlation length ζ. (b) The maximum intensity of the absorption spectrum $A_{\max}$ versus the generalized correlation length ζ. (c) By combining (a) and (b) we obtain the absorption spectrum intensity $A_{\max}$ versus the mean localization length $\lambda(E \approx 2)$.

ζ. We can combine Fig. 7(a) and (b) to provide the dependence of the maximum absorption spectrum intensity $A_{\max}$ versus the mean localization length $\lambda(E \approx 2)$ (see Fig. 7(c)). Our numerical results suggest that the maximum intensity of the absorption spectrum depends linearly on the localization length. We have considered other values of γ and no qualitative changes to the behavior of the maximum absorption spectrum were found. We would like to emphasize that we have also considered other values of ζ. Particularly we have computed the absorption spectrum for ζ up to 20 (results not shown here). In general, for ζ roughly larger than 1 the width σ_A of the absorption spectrum and the maximum absorption intensity $A_{\max}$ become roughly independent of ζ.

Our numerical calculations of the localization length explained the anomalous behavior of $A(E)$ in $1d$ models with stretched exponential correlated disorder. However, we will show another treatment of the optical properties based on a heuristic procedure. Our formalism is based on the topology of the eigenstates that contribute to the absorption spectrum. It is known that in a $1d$ disordered system with positive hopping the eigenstates with energy in the vicinity of $E \approx 2$ are those with the largest oscillator strength [35]. The high-energy range of the spectrum contains a hidden structure as was reported in Ref. [37]. The nature of states around $E \approx 2$ can be understood as a superposition of states of weakly coupled quantum wells of width λ. This feature reflects on a specific topology of those states; they display a topology similar to a bell. The states about $E \approx 2$ with bell shape are those with larger oscillator strength [35,39]. In Fig. 8 we can see a pedagogical picture of this kind of state. In a system with size N we will consider a localized bell shape state with width λ. Therefore, the wave function amplitude f_n is nonzero within the region of length λ and it is negligible for any another part of this $1d$ system. We will consider that $f_n = \mathcal{F} e^{(-|n-n_0|/\lambda)}$ within the region of size λ and $n_0 = 0$ as being the center of chain. Therefore, the normalization condition at the thermodynamic limit can be written as $\sum_{n=-N/2}^{N/2} f_n^2 \approx \int_{-N/2}^{N/2} \mathcal{F}^2 e^{(-2|n|/\lambda)} dn = 1$. After some

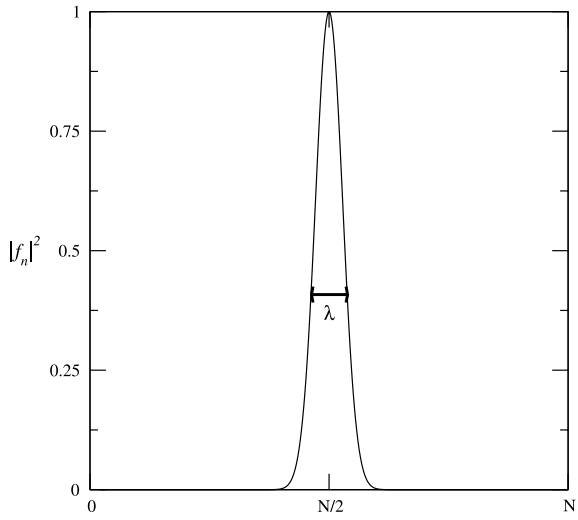

Fig. 8. Pedagogical picture of a localized bell shape state with width λ.

simple algebra we obtain $\mathcal{F} = [\sqrt{\lambda(1 - e^{-N/2\lambda})}]^{-1}$. Therefore, the oscillator strength F of this eigenstate can be written as $F = (\sum_{n=-N/2}^{N/2} f_n)^2 \approx (\int_{-N/2}^{N/2} \mathcal{F} e^{(-|n|/\lambda)} dn)^2 = \mathcal{F}^2 \lambda^2 (2 - 2e^{-N/2\lambda})^2$. The localization length λ at the high energy region ($E \approx 2$) is much smaller than the system size N; thus we can consider $e^{-N/\lambda} \to 0$ and $e^{-N/2\lambda} \to 0$. Therefore, at this limit the oscillator strength scales proportional to the localization length $F \propto \lambda$. This simple heuristic procedure corroborates our numerical calculations shown in Fig. 7(d) for the linear dependence of the intensity of the absorption spectrum on the localization length. We stress that in Ref. [33] it was pointed out that the oscillator strength is an inconvenient measure for the extension of the exciton states for the case of strong correlations. Therefore, we emphasize that our calculations should be valid only for small ζ.

4. Summary and conclusions

In this work we studied the problem of one-electron localization in $1d$ systems with correlated disorder as well as the optical absorption spectrum. We have considered chains with stretched exponential correlations on the diagonal disorder distribution ϵ_n. In order to impose these kinds of correlations we have considered the on-site energy ϵ_n proportional to $\sum_{m=1}^{N} \eta_m * \exp(-|n - m|^\gamma/\zeta)$ where η_m are uncorrelated random numbers and γ and ζ are tunable parameters that control the degree of correlations. We perform exact numerical diagonalization to compute the participation number and the absorption spectrum. Our formalism provides an estimate for the dependence of the localization length on the parameters γ and ζ. We analyzed the case with weak correlations ($\gamma \gg 1$ and $\zeta \to 0$) and also the case with strong correlations ($0 < \gamma < 1$ and $\zeta \gg 0$). Our calculations demonstrated that the weak correlated case exhibits a behavior similar to those obtained for the Anderson model with uncorrelated disorder. From another side, the strong correlated case reveals a new and interesting behavior. For $0 < \gamma < 1$, our calculations demonstrated that the localization length increases as the generalized correlation length ζ is increased. However, we have proved, by using a finite size scaling, that this model does not contain extended states. We also observe a non intuitive dependence of the localization properties on the exponent γ. For a fixed ζ we demonstrated that there is a particular interval $[\gamma_1, \gamma_2]$ in which the participation number and the localization length become almost of the same order of magnitude of the system size N. Therefore, our analysis provides the range of values of γ that promote higher electronic propagation. We used a spectral analysis of the correlated disorder and have explained the dependence of the participation number on the γ exponent. Our spectral analysis reveals that this kind of stretched exponential correlation behaves as a mechanism of smoothing of the internal roughness. Our results for the optical absorption spectra reveal an interesting dependence of the absorption profile on the correlated disorder distribution. We showed that as the generalized correlation length ζ is increased the absorption bandwidth increases linearly. Moreover, we also observed that the intensity of the absorption spectrum $A(E)$ also depends on the degree of correlations. We used a standard transfer matrix procedure and established numerically the direct relation between the absorption spectrum behavior and the localization length of those eigenstates that contribute to the absorption. We focused on the numerical calculation of the localization length λ of those eigenstates that contribute to the absorption band, and we have numerically demonstrated that the maximum intensity of the absorption spectrum $A_{\max}$ depends linearly on the localization length. Furthermore, we have used an analytical heuristic procedure based on the topology of those eigenstates. Our heuristic procedure corroborates the numerical prediction of the linearity between the intensity of the absorption spectrum and the localization length. In our calculations, we did not find a substantial dependence of the absorption spectrum on the γ exponent. In summary we have provided a detailed analysis of localization aspects and optical properties in chains with

stretched exponential correlations on the diagonal disorder distribution. We expect that the present work will stimulate further theoretical and experimental investigations along this line.

Acknowledgments

This work was partially supported by the Brazilian research agencies CNPq, CAPES, INCT-Nano(Bio)Simes, as well as FAPEAL (Alagoas State Agency). The research works of J.L.L. dos Santos and M.O. Sales were supported by a graduate program of CAPES.

References

[1] E. Abrahams, P.W. Anderson, D.C. Licciardello, T.V. Ramakrishnan, Phys. Rev. Lett. 42 (1979) 673.
[2] B. Kramer, A. MacKinnon, Rep. Prog. Phys. 56 (1993) 1469;
For a review see, e.g. I.M. Lifshitz, S.A. Gredeskul, L.A. Pastur, Introduction to the Theory of Disordered Systems, Wiley, New York, 1988.
[3] B. Kramer, K. Broderix, A. Mackinnon, M. Schreiber, Physica A 167 (1990) 163.
[4] R.A. Romer, H. Schulz-Baldes, Europhys. Lett. 68 (2004) 247.
[5] V.N. Kuzovkov, W. von Niessen, Physica A 377 (2007) 115.
[6] J. C. Flores, J. Phys.: Condens. Matter 1 (1989) 8471.
[7] D.H. Dunlap, H.L. Wu, P.W. Phillips, Phys. Rev. Lett. 65 (1990) 88;
H.-L. Wu, P. Phillips, Phys. Rev. Lett. 66 (1991) 1366.
[8] F.A.B.F. de Moura, M.L. Lyra, Phys. Rev. Lett. 81 (1998) 3735.
[9] F.A.B.F. de Moura, M.D. Coutinho-Filho, E.P. Raposo, M.L. Lyra, Europhys. Lett. 66 (2004) 585.
[10] I.F. dos Santos, F.A.B.F. de Moura, M.L. Lyra, M.D. Coutinho-Filho, J. Phys.: Condens. Matter. 19 (2007) 476213.
[11] F. Domínguez-Adame, V.A. Malyshev, F.A.B.F. de Moura, M.L. Lyra, Phys. Rev. Lett. 91 (2003) 197402.
[12] F.A.B.F. de Moura, Eur. Phys. J. B 78 (2010) 335.
[13] F.M. Izrailev, A.A. Krokhin, Phys. Rev. Lett. 82 (1999) 4062;
F.M. Izrailev, A.A. Krokhin, S.E. Ulloa, Phys. Rev. B 63 (2001) 41102.
[14] W.S. Liu, T. Chen, S .J. Xiong, J. Phys.: Condens. Matter 11 (1999) 6883.
[15] G.P. Zhang, S.-J. Xiong, Eur. Phys. J. B 29 (2002) 491.
[16] V. Bellani, E. Diez, R. Hey, L. Toni, L. Tarricone, G.B. Parravicini, F. Domínguez-Adame, R. Gómez-Alcalá, Phys. Rev. Lett. 82 (1999) 2159.
[17] V. Bellani, E. Diez, A. Parisini, L. Tarricone, R. Hey, G.B. Parravicini, F. Domínguez-Adame, Physica E 7 (2000) 823.
[18] H. Shima, T. Nomura, T. Nakayama, Phys. Rev. B 70 (2004) 075116.
[19] U. Kuhl, F.M. Izrailev, A. Krokhin, H.J. Stöckmann, Appl. Phys. Lett. 77 (2000) 633.
[20] H. Cheraghchi, S.M. Fazeli, K. Esfarjani, Phys. Rev. B 72 (2005) 174207.
[21] G. Schubert, A. Weiße, H. Fehske, Physica B 801 (2005) 359.
[22] F.M. Izrailev, A.A. Krokhin, N.M. Makarov, Phys. Rep. 512 (2012) 125–254.
[23] Rabah Benhenni, Khaled Senouci, Rachid Bouamrane, Nouredine Zekri, Physica A 389 (2010) 1002.
[24] W.W. Cheng, J.X. Li, C.J. Shan, L.Y. Gong, S.M. Zhao, Physica A 398 (2014) 1.
[25] G. Long-Yan, T. Pei-Qing, Z. Zi-Cong, Chin. Phys. B. 20 (2011) 087102.
[26] A. Croy, M. Schreiber, Phys. Rev. B 85 (2012) 205147.
[27] C. Albrecht, S. Wimberger, Phys. Rev. B 85 (2012) 045107.
[28] M.O. Sales, S.S. Albuquerque, F.A.B.F. de Moura, J. Phys.: Condens. Matter 24 (2012) 495401.
[29] M.O. Sales, F.A.B.F. de Moura, Physica E 45 (2012) 97.
[30] G.M. Petersen, N. Sandler, Phys. Rev. B 87 (2013) 195443.
[31] M. Hilke, Phys. Rev. A 80 (2009) 063820;
A. Crisanti, J. Phys. A 23 (1990) 5235.
[32] A. Rodríguez, V.A. Malyshev, F. Domínguez-Adame, J. Lumin. 131 (1999) 83–84.
[33] V.A. Malyshev, A. Rodríguez, F. Domínguez-Adame, Phys. Rev. B 60 (1999) 14140.
[34] F. Domínguez-Adame, V.A. Malyshev, A. Rodríguez, Chem. Phys. 244 (1999) 351.
[35] E. Díaz, A. Rodríguez, F. Domínguez-Adame, V.A. Malyshev, Europhys. Lett. 72 (2005) 1018.
[36] H. Fidder, J. Knoester, D.A. Wiersma, J. Chem. Phys. 95 (1991) 7880.
[37] V.A. Malyshev, J. Lumin. 55 (1993) 225–230.
[38] F. Domínguez-Adame, Phys. Rev. B 51 (1995) 12801.
[39] T.F. Assunção, M.L. Lyra, F.A.B.F. de Moura, F. Domínguez-Adame, Phys. Lett. A 375 (2011) 1048.
[40] A. Eisfeld, S.M. Vlaming, V.A. Malyshev, J. Knoester, Phys. Rev. Lett. 105 (2010) 137402.
[41] A. Werpachowska, A. Olaya-Castro, Phys. Rev. Lett. 109 (2012) 259701;
A. Eisfeld, S.M. Vlaming, V.A. Malyshev, J. Knoester, Phys. Rev. Lett. 109 (2012) 259702.
[42] A.V. Malyshev, V.A. Malyshev, F. Domínguez-Adame, J. Lumin. 129 (2009) 1779.
[43] E.M. Nascimento, F.A.B.F. de Moura, M.L. Lyra, Photon. Nanostruct. Fundamentals Appl. 7 (2009) 101–107.
[44] E. Macia, Rep. Prog. Phys. 69 (2006) 397.
[45] S. Russ, S. Havlin, I. Webman, Phil. Mag. B 77 (1998) 1449.